SPINT2 inhibits relevant proteases *in vitro* and *in vivo* required for activation of both influenza viruses and metapneumoviruses

Marco R. Straus[a], Jonathan T. Kinder[b], Michal Segall[a], Rebecca Ellis Dutch[b] and Gary R. Whittaker[a]

[a]Department of Microbiology and Immunology, College of Veterinary Medicine, Cornell University, Ithaca, New York, United States

[b]Department of Molecular and Cellular Biochemistry, University of Kentucky, Lexington, KY, United States.

Running Head: SPINT2 inhibits influenza virus and metapneumoviruses activation

#Address correspondence to Rebecca E. Dutch, rebecca.dutch@uky.edu or Gary R. Whittaker, gary.whittaker@cornell.edu

M.R.S and J.T.K contributed equally to this work

Abstract

Viruses that possess class I fusion proteins require proteolytic activation by host cell proteases to mediate fusion with the host cell membrane, which is a crucial step in infection. The mammalian SPINT2 gene encodes a protease inhibitor that inhibits a range of trypsin-like serine proteases, including those known to act on class I fusion proteins. Here we show the protease inhibitor SPINT2 restricts cleavage-activation with high efficacy, for a range of influenza viruses and for human metapneumovirus, and for cleavage via a series of functionally-relevant proteases: namely trypsin, recombinant matriptase, kallikrein-related

peptidases (KLK) 5 & 12, human-airway trypsin-like protease (HAT) and plasmin. SPINT2 inhibitor treatment resulted in the cleavage and fusion inhibition of full-length influenza A/Ca/04/09 (H1N1) HA, A/Aichi/68 (H3N2) HA and A/Shanghai/2/2013 (H7N9) HA when activated by trypsin, recombinant matriptase or KLK5. For HMPV, SPINT2 inhibitor was also able to block cleavage of F by trypsin, KLK5 and matriptase. We also demonstrate that SPINT2 inhibitor was able to reduce viral growth of influenza A/Ca/04/09 H1N1 and A/X31 H3N2 in cell culture by inhibiting matriptase or TMPRSS2. Moreover, inhibition efficacy did not differ whether SPINT2 was added at the time of infection or 24 hours post-infection. Our data suggest that the SPINT2 inhibitor has a strong potential to serve as a novel antiviral therapy with a broad spectrum.

Importance

Respiratory viruses such as influenza A and HMPV infect millions of people each year resulting in a vast number of hospitalizations and high mortality rates. Current treatments against influenza include yearly vaccines and antiviral therapies targeting viral specific factors. Both vaccines and antiviral therapies are challenged by emerging virus strains that are resistant to these treatments. To date, there are no effective treatments available for HMPV infections. Here, we describe SPINT2, a protease inhibitor that targets trypsin-like serine host proteases which are responsible for the activation of influenza and HMPV fusion proteins. The fact that SPINT2 acts against host cell factors limits the possibility of emerging resistance phenotypes in virus strains. Given that other respiratory viruses such as MERS and SARS can be activated by similar proteases, SPINT2 could be developed into a broad-spectrum antiviral therapy against respiratory viruses that utilize class I fusion proteins.

Introduction

Influenza-like illnesses (ILIs) represent a significant burden on public health and can be caused by a range of respiratory viruses in addition to influenza virus itself (1). An ongoing goal of anti-viral drug discovery

is to develop broadly-acting therapeutics that can be used in the absence of definitive diagnosis, such as in the case of ILIs. For such strategies to succeed, drug targets that are shared across virus families need to be identified.

One common cause of ILI are influenza A viruses, including H1N1 and H3N2, that cross species barriers from their natural avian hosts and infect humans (2, 3). Novel emerging viruses such as H7N9 that has caused hundreds of deaths since its appearance in China in 2013 pose an additional concern (4). The World Health Organization (WHO) estimates that each year about 1 billion suffer from flu infections, 3 to 5 million people worldwide are hospitalized with severe illness and approximated 290,000 to 650,000 people die from the disease (5). Mortality rates dramatically rise during influenza pandemics as observed with the Spanish flu of 1918, the Asian pandemic of 1957 and the Hong Kong pandemic of 1968 (3, 6). Vaccinations can provide an effective protection against seasonal and pandemic outbreaks but provide limited or no protection when viruses evolve and/or acquire mutations resulting in antigenically distinct viruses. This antigenic drift or shift requires that new vaccines be produced quickly and in vast amounts which can be problematic especially during pandemics. In addition to vaccines, several antiviral therapies have been applied to treat influenza A infections such as adamantanes acting as M2 ion channel blockers (amantadine, rimantadine) and neuraminidase inhibitors which block the cleavage of sialic acid in newly formed virions (oseltamivir, zanamivir) (7). However, several influenza subtypes including the most common H1N1 and H3N2 have emerged globally that are resistant against adamantanes and similar observations were made with respect to oseltamivir (7).

Another common cause of ILI is pneumo- and paramyxoviruses, including human metapneumovirus (HMPV), respiratory syncytial virus, and parainfluenza viruses. Clinical presentation of these viruses resembles many of the symptoms of influenza and they cause significant morbidity and mortality as well as a large economic burden (8, 9). HMPV is ubiquitous, with nearly everyone infected by the age of 5 and reinfection is common throughout life impacting children, elderly and immunocompromised individuals

(10–12). While HMPV is a common cause of ILI, there are currently no approved vaccines or antiviral therapeutics. Further research is needed to establish targets for intervention and factors required for infection need to be examined in more detail.

Some influenza viruses and HMPV appear to share common activating proteases. The influenza fusion protein hemagglutinin (HA) is synthesized as a precursor that needs to be cleaved by host cell proteases to exert its fusogenic activity (13, 14). Cleavage separates the precursor HA_0 into HA_1 and HA_2 which remain associated via disulfide bonds and leads to exposure of the fusion peptide at the N-terminus of HA_2 (13, 14). Low pathogenicity avian influenza (LPAI) usually possess a monobasic cleavage site which consists of 1 – 2 non-consecutive basic amino acids and which is generally cleaved by trypsin-like serine proteases such trypsin, and members of the type II transmembrane serine proteases (TTSP) including TMPRSS2, TMPRSS4, HAT (TMPRSS11D) and matriptase (13–15). In addition, some other proteases such as KLK5 and KLK 12 have been implicated in influenza pathogenicity (16). In humans these proteases are localized in the respiratory tract and therefore influenza infections are usually confined to this tissue. In contrast, highly pathogenic avian influenza (HPAI) viruses are defined by a polybasic cleavage site which consists of 6 – 7 basic residues allowing them to be activated by members of the proprotein convertase (PC) family such as furin and PC6 (17). These proteases are not confined to a specific tissue and dramatically increase the risk of a systemic infection.

Similar to influenza HA, HMPV requires the fusion protein (F) to be proteolytically processed at a single basic residue to generate the active, metastable form. Without this cleavage process, the F protein is unable to mediate viral entry into the target cell. However, to date, only trypsin and TMPRSS2 have been shown to effectively cleave HMPV F and other proteases have yet to be identified (18, 19).

In addition, other respiratory viruses have been reported to utilize similar proteases for activation, including SARS and MERS, demonstrating that targeting these proteases would inhibit multiple respiratory pathogens (20). The fact that proteolytic activation is such a crucial step for several respiratory viruses

that predominately require a specific class of proteases makes these proteases a viable target for the development of novel antiviral therapies (21). Earlier studies described the administration of the serine protease inhibitor aprotinin to inhibit influenza replication and demonstrated that aprotinin successfully inhibited IAV activation and replication (22). However, when targeting host specific factors there are potential off target effects, and therefore the potential side effects of targeting host proteases requires further investigation. Hamilton et al. reported that the hepatocyte growth activator inhibitor 2 (HAI-2) effectively inhibited trypsin-mediated cleavage of H1N1 and H3N2 *in vitro* and *in vivo* (23). HAI-2 is encoded by the SPINT2 gene and hereafter we will also refer to the protein as SPINT2. SPINT2 is plasma membrane-localized serine protease inhibitor that is found in various tissues including the respiratory tract (24). Recent reports associated the physiological role of SPINT2 with the inhibition of serine-type proteases such as matriptase and plasmin and that deregulation of SPINT2 inhibition is suggested to play a role in cancer development and progression (25–27). SPINT2 possesses two kunitz-type inhibitor domains that are exposed to the extracellular space and which are believed to facilitate a potent inhibition of target proteases. Wu et al. recently described that the kunitz-type domain 1 of SPINT2 is responsible for matriptase inhibition (25).

A previous study from our lab described the effective inhibition of trypsin by SPINT2 resulting in dramatically reduced cleavage of influenza A HA and subsequent reduced viral growth in cell culture and mouse studies (23). Here, we report that purified SPINT2 protein inhibits several human host proteases such as matriptase and TMPRSS2 that are relevant for the activation of significant influenza viruses currently circulating and causing disease outbreaks. We also tested the potential of SPINT2 to inhibit the activation of the fusion protein (F) from human metapneumovirus (HMPV), a member of the pneumovirus family. We confirm the original findings that HMPV F is proteolytically processed by trypsin and TMPRSS2. In addition, we found that HAT, KLK5 and matriptase were able to cleave F, but KLK12 could not. Our results show that SPINT2 can inhibit the activation of proteases that are responsible for the activation of

121 influenza H1N1, H3N2 and H7N9 HA as well as HMPV F. In a cell culture model, we demonstrate that viral
122 loads are significantly reduced in the presence of SPINT2 when infections were conducted with
123 A/Ca/04/09 and A/X31. Moreover, the application of SPINT2 24 hours post infection inhibited the
124 activation of influenza A viruses with the same efficacy as when SPINT2 was added to cell culture medium
125 at the time of infection. Thus, SPINT2 exhibits the potential to serve as a novel and efficient antiviral
126 therapeutic to relieve patients from influenza A, human metapneumovirus, SARS and potentially other
127 respiratory viruses that require these host factors for entry.

128 **Results**

129 **SPINT2 inhibits recombinant human respiratory tract proteases that cleave HA cleavage site peptide**
130 **mimics**

131 We previously tested the ability of SPINT2 to inhibit proteases shown to cleave HAs from seasonal and
132 pandemic influenza A strains that infected humans by using a fluorogenic peptide cleavage assay that
133 utilizes fluorogenic peptides mimicking the HA cleavage site (28, 29). We found that certain HA subtypes
134 such as H1, H2 and H3 are cleaved by a wide variety of human respiratory proteases while others such H5,
135 H7 and H9 displayed more variability in cleavage by proteases and seemed less well adapted to proteases
136 present in the human respiratory tract (29). Here, we extended our previous study and tested a peptide
137 mimicking the cleavage site of the pneumovirus fusion protein of HMPV F with a variety of proteases for
138 their ability to cleave the peptide mimic (Figure 1) (19, 30). When we tested cleavage of a peptide
139 mimicking the HMPV F cleavage site by trypsin, matriptase, KLK5, KLK12, HAT and plasmin we found that
140 all proteases except KLK12 were able to proteolytically cleave the peptide (Figure 1). However, the Vmax
141 values for matriptase (9.24 nM), KLK5 (5.8 nM) and HAT (2.99 nM) were very low compared to trypsin
142 (135.2) suggesting that the three proteases have a lower affinity interaction and processivity for HMPV F.
143 Next, trypsin, matriptase and KLK5 were selected for the SPINT2 inhibition assays as described below.

For the SPINT2 inhibition assays, trypsin which typically resides in the intestinal tract and expresses a very broad activity towards different HA subtypes and HMPV F served as a control (31). We measured the Vmax values for each protease/peptide combination in the presence of different SPINT2 concentrations and plotted the obtained Vmax values against the SPINT2 concentrations on a logarithmic scale (Supplementary Figure 1). Using Prism7 software, we then determined the IC_{50} that reflects at which concentration the V_{max} of the respective reaction is inhibited by half. SPINT2 cleavage inhibition of a representative H1N1 cleavage site by trypsin results in an IC50 value of 70.6 nM (Table 1A) while the inhibition efficacy of SPINT2 towards matriptase, HAT, KLK5 and KLK12 ranged from 11 nM to 25 nM (Table 1A). However, inhibition was much less efficient for plasmin compared with trypsin (122 nM). We observed a similar trend when testing peptides mimicking the H3N2 and H7N9 HA cleavage sites using trypsin, HAT, KLK5, plasmin and trypsin, matriptase, plasmin, respectively (Table 1A). With the exception of plasmin, we found that human respiratory tract proteases are inhibited with a higher efficacy compared to trypsin. We expanded our analysis to peptides mimicking HA cleavage sites of H2N2, H5N1 (LPAI and HPAI), H6N1 and H9N2 that all reflected the results described above (Table 1A). Only cleavage inhibition of H6N1 HA by KLK5 did not significantly differ from the observation made with trypsin (Table 1A).

When we tested inhibition of HMPV cleavage by trypsin, matriptase and KLK5. SPINT2 showed a very high inhibition efficacy for all three tested proteases with measured IC50s for trypsin, matriptase and KLK5 of 0.04 nM, 0.0003 nM and 0.95 nM, respectively (Table 1B).Compared to the IC50 values observed with the peptides mimicking influenza HA cleavage site motifs the IC50 values for the HMPV F peptide were very low.

Cleavage of distinct full-length HA subtypes is efficiently inhibited by SPINT

Cleavage of peptides mimicking a HA cleavage site does not always reflect the *in vivo* situation and requires validation by expressing the full-length HA protein in a cell culture model to test cleavage and cleavage inhibition of the respective protease (29). However, before conducting these experiments we

wanted to ensure that SPINT2 does not have a cytotoxic effect on cells. Therefore, 293T cells were incubated with various concentrations of SPINT2 over a time period of 24 hours. PBS and 500µM H_2O_2 served as cytotoxic negative and positive controls respectively. We did not observe any cytotoxicity with any of the tested SPINT2 concentrations (Figure 2).

To test SPINT2-mediated cleavage inhibition of full-length HA we expressed the HAs of A/Ca/04/09 (H1N1), A/x31 (H3N2) and A/Shanghai/2/2013 (H7N9) in 293T cells and added recombinant matriptase or KLK5 protease that were pre-incubated with 10nM or 500nM SPINT2. Trypsin and the respective protease without SPINT2 incubation were used as controls. Cleavage of HA_0 was analyzed via Western Blot and the signal intensities of the HA_1 bands were quantified using the control sample without SPINT2 incubation as a reference point (Figure 3A and 3B-D). Trypsin cleaved all tested HA proteins with very high efficiency that was not observed with matriptase or KLK5 (Figure 3B-D). However, H1N1 HA was cleaved by matriptase and KLK5 to a similar extent without and with 10nM SPINT2. 500nM SPINT2 led to a cleavage reduction of about 70% and 50% for matriptase and KLK5, respectively (Figure 3A and 3B). KLK5-mediated cleavage of H3N2 HA was reduced by about 10% when KLK5 was pre-incubated with 10nM SPINT2 and by about 60% when 500nM SPINT2 was used (Figure 3A and 3C). When we tested the cleavage inhibition of matriptase with H7N9 HA as a substrate we found that 10nM and 500nM SPINT reduced the cleavage to 40% and 10% cleavage respectively compared to the control. (Figure 3A and 3D). In contrast, 10nM SPINT2 had no effect on KLK5-mediated cleavage of H7N9 HA while 500nM reduced cleavage by approximately 70% (Figure 3A and 3D).

Next, we examined which proteases in addition to trypsin and TMPRSS2 were able to cleave HMPV F. First, we co-transfected the full length TMPRSS2, HAT and matriptase with HMPV F in VERO cells. The F protein was then radioactively labeled with ^{35}S methionine and cleavage was examined by quantifying the F_0 full length protein and the F_1 cleavage product. We found that TMPRSS2 and HAT were able to efficiently cleave HMPV F while matriptase decreased the expression of F, though it is not clear if this was due to

general degradation of protein or lower initial expression. However, matriptase demonstrated potential low-level cleavage when co-transfected (Figure 4A and B). We then examined cleavage by the exogenous proteases KLK5, KLK12 and matriptase. Compared with the trypsin control, KLK5 and matriptase were able to cleavage HMPV F, while KLK12 was not (Figure 4C and D). In agreement with the peptide assay, cleavage of HMPV F by KLK5 and matriptase was less efficient than trypsin and both peptide and full length protein assays demonstrate that KLK12 does not cleave. This also serves as confirmation that matriptase likely cleaves HMPV F, but co-expression with matriptase may alter protein synthesis, stability or turnover if co-expressed during synthesis and transport to the cell surface. Next, we tested SPINT2 inhibition of exogenous proteases trypsin, KLK5 and matriptase. We pre-incubated SPINT2 with each protease and added it to VERO cells expressing HMPV F and analyzed cleavage product formation. SPINT2 pre-incubation minimally affected cleavage at 10nm but 500nm resulted in inhibition of trypsin, KLK5 and matriptase cleavage of HMPV, similar to our findings for HA (Figure 4E and F).

We also tested whether cleavage inhibition by SPINT2 resulted in the inhibition of cell fusion. As described above, matriptase and KLK5 were pre-incubated with 10nM and 500nM SPINT2 and subsequently added to VERO cells expressing A/Ca/04/09 (H1N1) HA or A/Shanghai/2/2013 (H7N9) HA. Cells were then briefly exposed to a low pH buffer to induce fusion and subsequently analyzed using an immune fluorescence assay. When matriptase and KLK5 were tested with 10nM SPINT2 and incubated with VERO cells expressing H1N1 HA we still observed syncytia formation (Figure 5A). However, 500mM SPINT2 resulted in the abrogation of syncytia formation triggered by cleavage of the respective HA by matriptase and KLK5. We made the same observation when we tested KLK5 and H7N9 HA (Figure 5B). Matriptase-mediated H7N9 HA syncytia formation was inhibited by the addition of 10nM SPINT2 (Figure 5B).

SPINT2 reduces viral growth in cell culture

To understand whether SPINT2 was able to inhibit or reduce the growth of live virus in a cell culture model over the course of 24 hours we transfected cells with human TMPRSS2 and human matriptase, two major

proteases that have been shown to be responsible for the activation of distinct influenza A subtype viruses. TMPRSS2 is essential for H1N1 virus propagation in mice and plays a major role in the activation of H7N9 and H9N2 viruses (32–34). Matriptase cleaves H1N1 HA in a sub-type specific manner, is involved in the *in vivo* cleavage of H9N2 HA and our results described above suggest a role for matriptase in the activation of H7N9 (16, 34). At 18 hours post transfection we infected MDCK cells with A/Ca/04/09 (H1N1) at a MOI of 0.1 and subsequently added SPINT2 protein at different concentrations. Non-transfected cells served as a control and exogenous trypsin was added to facilitate viral propagation. SPINT2 initially mitigated trypsin-mediated growth of H1N1 at a concentration of 50nM and the extent of inhibition slightly increased with higher concentrations (Figure 6A, Table 2A). The highest tested SPINT2 concentration of 500nM reduced viral growth by about 1 log (Figure 6A, Table 2A). We observed a similar pattern with cells transfected with human matriptase (Figure 6B, Table 2A). Growth inhibition started at a SPINT2 concentration of 50nM and with the application of 500nM growth was reduced by approximately 1.5 logs (Figure 6B, Table 2A). When we infected cells expressing TMPRSS2 with H1N1 and added SPINT2, viral growth was significantly reduced at a concentration of 150nM. Addition of 500nM SPINT2 led to a reduction of viral growth of about 1.5 logs (Figure 6C, Table 2A). We also tested whether SPINT2 could reduce the growth of a H3N2 virus because it is major circulating seasonal influenza subtype. However, TMPRSS2 and matriptase do not seem to activate H3N2 viruses (16, 35). Hence, trypsin and SPINT2 were added to the growth medium of cells infected with A/X31 H3N2. Compared to control cells without added inhibitor SPINT2 significantly inhibited trypsin-mediated H3N2 growth at a concentration of 50nM (Figure 6D, Table 2A). At the highest SPINT2 concentration of 500nM viral growth was reduced by about 1 log (Figure 6D).

Antiviral therapies are often applied when patients already show signs of disease. Therefore, we tested if SPINT2 was able to reduce viral growth when added to cells 24 hours after the initial infection. Cells were infected with 0.1 MOI of A/Ca/04/09 (H1N1) and trypsin was added to promote viral growth. At the time

of infection, we also added 500nM SPINT2 to one sample. A second sample received 500nM SPINT2 24 hours post infection. Growth supernatants were harvested 24 hours later, and viral growth was analyzed. We found that viral growth was reduced by 1 log regardless whether SPINT2 was added at the time of infection or 24 hours later (Figure 7, Table 2B).

Discussion

Influenza A has caused four pandemics since the early 20th century and infects millions of people each year as seasonal flu resulting in up to 690,000 deaths annually (5). Vaccination efforts have proven to be challenging due to the antigenic drift of the virus and emerging resistance phenotypes (36). Moreover, the efficacy of vaccines seems to be significantly reduced in certain high-risk groups (37). Prevalent antiviral therapies to treat influenza A-infected patients such as adamantanes and neuraminidase inhibitors target viral proteins but there is increasing number of reports about circulating influenza A subtypes that are resistant to these treatments (7). In this study we focused on a novel approach that uses antiviral therapies targeting host factors rather than viral proteins offering a more broad and potentially more effective therapeutic approach (21). We demonstrate that SPINT2, a potent inhibitor of serine-type proteases, is able to significantly inhibit cleavage of HA, impair the fusion of cells and hence, reduce viral growth *in vivo*.

SPINT2 demonstrates greater advantage over other inhibitors of host proteases such as e.g. aprotinin that was shown to be an effective antiviral but also seemed to be specific only for a subset of proteases (22). Our peptide assay suggests that SPINT2 has a wide variety of host protease specificity. With the exception of plasmin, all the tested proteases in combination with peptides mimicking the cleavage site of different HA subtypes expressed IC_{50} values in the nanomolar range. Interestingly, the IC50 values obtained for cleavage inhibition of HMPV F were substantially lower, in the picomolar range. This suggests that the HMPV cleavage may be more selectively inhibited by SPINT2. However, the western blot data showed that addition of the lowest concentration (10 nM) of SPINT2 did not result in cleavage inhibition of HMPV

F by the tested proteases. Differences in sensitivity of SPINT2 between influenza HA and HMPV require further investigation.

SPINT2 poses several potential advantages over other inhibitors that target host proteases. Cell culture studies showed that, for example, matriptase-mediated H7N9 HA cleavage was efficiently inhibited at a concentration of 10nM SPINT2. In contrast, the substrate range for aprotinin, a serine protease inhibitor shown to reduce influenza A infections by targeting host proteases, seemed to be more limited (22). Other synthetic and peptide-like molecules designed to inhibit very specific serine proteases such as TMPRSS2, TMPRSS4 and TMPRSS11D (HAT) were only tested with those proteases and their potential to inhibit other proteases relevant for influenza A activation remains unclear (38–40). However, when we tested the potential of SPINT2 to inhibit viral replication in a cell culture model we were only able to achieve growth reductions of approximately 1 -1.5 logs after 48 hours with a concentration of 500nM SPINT2. One potential explanation is that 500nM SPINT2 was unable to saturate the proteases present in the individual experiments and was not sufficient to prevent viral growth. In addition, the continuous overexpression of matriptase and TMPRSS2 may have produced an artificially high quantity of protein that exceeded the inhibitory capacities of SPINT2. This problem could be solved either by using higher concentration of SPINT2 or by optimizing its inhibitory properties. SPINT2 did not express any cytotoxic effects up to a concentration of 10mM. In comparison with other studies, the SPINT2 concentration we used here were in the nanomolar range while other published inhibitors require micromolar concentrations (38–40). However, we believe that future research will allow to fully exploit the potential of SPINT2 as a broad-spectrum antiviral therapy. Wu et al., recently described that the Kunitz domain I of SPINT2 is responsible for the inhibition of matriptase (25). In future studies we will explore whether the inhibitory capabilities of SPINT2 can be condensed into small peptides that may improve its efficacy. Its ability to inhibit a broad range of serine protease that are involved in the activation of influenza A suggest that a SPINT2 based antiviral therapy could be efficient against other pathogens too. TMPRSS2, for example, does not only

play a major role in the pathogenesis of H1N1 but is also required for the activation of SARS (Severe Acute Respiratory Syndrome) and MERS (Middle East Respiratory Syndrome) coronaviruses and HMPV (41, 42). Currently, treatment options for these viruses are very limited and therefore SPINT2 could become a viable option if its potential as an antiviral therapeutic can be fully exploited.

Materials and Methods

Cells, plasmids, viruses, and proteins

293T, VERO and MDCK cells (American Type Culture Collection) used for influenza experiments were maintained in Dulbecco's modified Eagle medium (DMEM) supplemented with 25 mM HEPES (Cellgro) and 10% fetal bovine serum (VWR). VERO cells used for HMPV experiments were maintained in DMEM (HyClone) supplemented with 10% FBS (Sigma). The plasmid encoding A/Ca/04/09 (H1N1) HA was generated as described (16). The plasmid encoding for HMPV F S175H434 was generated as described(43). The plasmids encoding for A/Shanghai/2/2013 (H7N9) HA, human TMPRSS2 and human matriptase were purchased from Sino Biological Inc. The plasmid encoding for A/Aichi/2/68 (H3N2) HA was generously donated by David Steinhauer. A/Ca/04/09 and A/X31 viruses were propagated in eggs. All recombinant proteases were purchased as described (29).

Expression and purification of SPINT2

SPINT2 was expressed and purified as described with minor modification (23). In brief, *E. coli* RIL (DE3) arctic express cells (Agilent) were transformed with SPINT2-pSUMO. Cells were then grown in 0.5 L Luria Broth containing 50 µg/ml kanamycin at 37°C. At OD 0.5-0.6 cells were chilled on ice and protein expression was induced with 0.2 mM IPTG. Cells were then grown over night at 16°C. Cells were harvested and protein was purified as previously described (23). SPINT2 protein was eluted by a 1-hour incubation with ULP1-6xHis. Glycerol was added to the eluted SPINT2 protein to a final concentration of 20% and protein aliquots were stored at -80°C. Protein concentration was determined by analyzing different dilutions of SPINT2 on an SDS-PAGE gel along with 5 defined concentrations of BSA between 100 ng and

1 µg. The gel was then stained with Coomassie, scanned with ChemiDoc Imaging system (Bio-Rad) and bands were quantified using Image Lab software (Bio-Rad). Concentrations of the SPINT2 dilutions were determined based on the BSA concentrations and the final SPINT2 concentration was calculated based on the average of the SPINT2 different dilutions.

Peptide Assays

Peptide assays were carried out as described (29). The sequence of the HMPV F peptide mimicking the HMPV F cleavage site used in this assay is ENPRQSRFVL including the same N- and C-terminal modifications as described for the HA peptides (29). The V_{max} was calculated by graphing each replicate in Microsoft Excel and determining the slope of the reaction for every concentration (0 nM, 1 nM, 5 nM, 10 nM, 25 nM, 50 nM, 75 nM, 150 nM, 300 nM and 500 nM). The V_{max} values were then plotted in the GraphPad Prism 7 software against the log10 of the SPINT2 concentration to produce a negative sigmoidal graph from which the IC_{50}, or the concentration of SPINT2 at which the V_{max} is inhibited by half, could be extrapolated for each peptide protease mixture. Since the x-axis was the log10 of the SPINT2 concentration, the inverse log was then taken for each number to calculate the IC_{50} in nM.

Cytotoxicity assay

The cytotoxicity assay was performed with a cell counting kit-8 (Dojindo Molecular Technologies) according to the manufacturer's instructions. In brief, approx. 2 x 10^3 293T cells were seeded per well of a 96-well plate and grown over night. SPINT2 was added at the indicated concentrations. DMEM and 500 µM H_2O_2 were used as a control. 24 hours later 10 µl CKK-8 solution were added to each well and incubated for 1 hour. Absorbance at 450 nm was measured using a SPARK microplate reader (Tecan). Per sample and treatment three technical replicates were used and the average was counted as one biological replicate. Experiment was conducted three times.

Metabolic protein labeling and immunoprecipitation of HMPV fusion protein

335 VERO cells were transfected with 2ug of pDNA using Lipofectamine and plus reagent (Invitrogen) in opti-
336 mem (Gibco) according to the manufacturers protocol. The following day, cells were washed with PBS and
337 starved in cysteine/methionine deficient media for 45 min and radiolabeled with 50uC/mL S35-
338 cysteine/methionine for 4 hours. Cells were lysed in RIPA lysis buffer and processed as described
339 previously (19) and the fusion protein of HMPV was immunoprecipitated using anti-HMPV F 54G10
340 monoclonal antibody (John Williams, U. Pitt). Samples were run on a 15% SDS-PAGE and visualized using
341 the typhoon imaging system. Band densitometry was conducted using ImageQuant software (GE).

342 **SPINT2 cleavage inhibition by Western blot and cell-cell fusion assay**

343 Experiments were performed as previously described with minor modifications (23). Treatment with
344 trypsin, recombinant matriptase and KLK5 were conducted as described (16, 44). For western blot analysis
345 293T cells were transfected with Turbofect (Invitrogen) according to manufacturer's instructions. Cell-cell
346 fusion assays were conducted with Vero cells that were transfected with Lipofectamine according to the
347 manufacturer's instructions. Antibodies to detect A/Ca/04/09 (H1N1) HA (NR28666), A/Aichi/2/68 (H3N2)
348 HA (NR3118) and A/Shanghai/2/2013 (H7N9) HA (NR48765) were obtained from the Biodefense and
349 Emerging Infections Research Resources Repository. Respective secondary antibodies had an Alexa488
350 tag (Invitrogen). Western blot membranes were scanned using a ChemiDoc imaging system (Bio-Rad). For
351 quantification the pixel intensity of the individual HA_1 bands was measured using ImageJ software and
352 cleavage efficiencies were calculated by the following equation: HA_1 10 nM or 500 nM SPINT2/HA_1 0nM
353 SPINT2 x 100%. Cell-cell fusion assays were carried out as described (16).

354 **Inhibition of viral infection in cell culture**

355 MDCK cells were seeded to a confluency of about 70% in 6-well plates. One plate each was then
356 transformed with a plasmid allowing for the expression of human matriptase or human TMPRSS2. One
357 plate was transformed with empty vector. 18 hours post transfection cells were infected with the
358 respective egg-grown virus at a MOI of approx. 0.1. Different SPINT2 concentrations were added as

359 indicated. 0.8 nM trypsin was added to the cells transformed with the empty vector. 48 hours post
360 infection supernatants were collected, centrifuged and stored at -80°C. Viral titers were determined using
361 an immune-plaque assay as described (45).

362 **Acknowledgements**

363 J.T.K. and R.E.D. thank Dr. John Williams form U.Pitt Children's Hospital for kindly providing the 54G10
364 anti-HMPV F antibody. This work was funded by National Institutes of Health grant 5R21AI117300.

365 **References**

366 1. World Health Organization. 2001. Global Epidemiological Surveillance Standards for Influenza 43.
367 2. Fouchier RAM, Guan Y. 2013. Ecology and evolution of influenza viruses in wild and domestic
368 birds. Textb Influ 173–189.
369 3. Yen H, Webster RG. 2009. Pandemic Influenza as a Current Threat, p. 3–24. *In* Current Topics in
370 Microbiology and Immunology.
371 4. The World Health Organization. 2017. WHO | Human infection with avian influenza A(H7N9)
372 virus – China. WHO.
373 5. WHO. 2018. Influenza fact sheet. World Heal Organ.
374 6. Kilbourne ED. 2006. Influenza pandemics of the 20th century. Emerg Infect Dis 12:9–14.
375 7. Hussain M, Galvin HD, Haw TY, Nutsford AN, Husain M. 2017. Drug resistance in influenza a virus:
376 The epidemiology and management. Infect Drug Resist 10:121–134.
377 8. Taylor S, Lopez P, Weckx L, Borja-Tabora C, Ulloa-Gutierrez R, Lazcano-Ponce E, Kerdpanich A,
378 Angel Rodriguez Weber M, Mascareñas de Los Santos A, Tinoco J-C, Safadi MAP, Lim FS,
379 Hernandez-de Mezerville M, Faingezicht I, Cruz-Valdez A, Feng Y, Li P, Durviaux S, Haars G, Roy-
380 Ghanta S, Vaughn DW, Nolan T. 2017. Respiratory viruses and influenza-like illness: Epidemiology
381 and outcomes in children aged 6 months to 10 years in a multi-country population sample. J
382 Infect 74:29–41.

383 9. Li Y, Reeves RM, Wang X, Bassat Q, Brooks WA, Cohen C, Moore DP, Nunes M, Rath B, Campbell
384 H, Nair H, Acacio S, Alonso WJ, Antonio M, Ayora Talavera G, Badarch D, Baillie VL, Barrera-
385 Badillo G, Bigogo G, Broor S, Bruden D, Buchy P, Byass P, Chipeta J, Clara W, Dang D-A, de Freitas
386 Lázaro Emediato CC, de Jong M, Díaz-Quiñonez JA, Do LAH, Fasce RA, Feng L, Ferson MJ, Gentile
387 A, Gessner BD, Goswami D, Goyet S, Grijalva CG, Halasa N, Hellferscee O, Hessong D, Homaira N,
388 Jara J, Kahn K, Khuri-Bulos N, Kotloff KL, Lanata CF, Lopez O, Lopez Bolaños MR, Lucero MG,
389 Lucion F, Lupisan SP, Madhi SA, Mekgoe O, Moraleda C, Moyes J, Mulholland K, Munywoki PK,
390 Naby F, Nguyen TH, Nicol MP, Nokes DJ, Noyola DE, Onozuka D, Palani N, Poovorawan Y, Rahman
391 M, Ramaekers K, Romero C, Schlaudecker EP, Schweiger B, Seidenberg P, Simoes EAF, Singleton
392 R, Sistla S, Sturm-Ramirez K, Suntronwong N, Sutanto A, Tapia MD, Thamthitiwat S, Thongpan I,
393 Tillekeratne G, Tinoco YO, Treurnicht FK, Turner C, Turner P, van Doorn R, Van Ranst M, Visseaux
394 B, Waicharoen S, Wang J, Yoshida L-M, Zar HJ. 2019. Global patterns in monthly activity of
395 influenza virus, respiratory syncytial virus, parainfluenza virus, and metapneumovirus: a
396 systematic analysis. Lancet Glob Heal 7:e1031–e1045.
397 10. Kahn JS. 2006. Epidemiology of Human Metapneumovirus. Clin Microbiol Rev 19:546–557.
398 11. van den Hoogen BG, de Jong JC, Groen J, Kuiken T, de Groot R, Fouchier RAM, Osterhaus ADME.
399 2001. A newly discovered human pneumovirus isolated from young children with respiratory
400 tract disease. Nat Med 7:719–724.
401 12. Leung J, Esper F, Weibel C, Kahn JS. 2005. Seroepidemiology of Human Metapneumovirus (hMPV)
402 on the Basis of a Novel Enzyme-Linked Immunosorbent Assay Utilizing hMPV Fusion Protein
403 Expressed in Recombinant Vesicular Stomatitis Virus. J Clin Microbiol 43:1213–1219.
404 13. Steinhauer D. 1999. Role of hemagglutinin cleavage for the pathogenicity of influenza virus.
405 Virology 258:1–20.
406 14. Taubenberger JK. 1998. Influenza virus hemagglutinin cleavage into HA1, HA2: no laughing

matter. Proc Natl Acad Sci U S A 95:9713–9715.

15. Böttcher-Friebertshäuser E, Klenk HD, Garten W. 2013. Activation of influenza viruses by proteases from host cells and bacteria in the human airway epithelium. Pathog Dis 69:87–100.

16. Hamilton BS, Whittaker GR. 2013. Cleavage activation of human-adapted influenza virus subtypes by kallikrein-related peptidases 5 and 12. J Biol Chem 288:17399–17407.

17. Horimoto T, Nakayama K, Smeekens SP, Kawaoka Y. 1994. Proprotein-processing endoproteases PC6 and furin both activate hemagglutinin of virulent avian influenza viruses. J Virol 68:6074–6078.

18. Shirogane Y, Takeda M, Iwasaki M, Ishiguro N, Takeuchi H, Nakatsu Y, Tahara M, Kikuta H, Yanagi Y. 2008. Efficient Multiplication of Human Metapneumovirus in Vero Cells Expressing the Transmembrane Serine Protease TMPRSS2. J Virol 82:8942–8946.

19. Schowalter RM, Smith SE, Dutch RE. 2006. Characterization of Human Metapneumovirus F Protein-Promoted Membrane Fusion: Critical Roles for Proteolytic Processing and Low pH. J Virol 80:10931–10941.

20. Millet JK, Whittaker GR. 2014. Host cell proteases: Critical determinants of coronavirus tropism and pathogenesis. Virus Res.

21. Laporte M, Naesens L. 2017. Airway proteases: an emerging drug target for influenza and other respiratory virus infections. Curr Opin Virol 24:16–24.

22. Zhirnov OP, Matrosovich TY, Matrosovich MN, Klenk H. 2011. Short communication Aprotinin , a protease inhibitor , suppresses proteolytic activation of pandemic H1N1v influenza virus 174:169–174.

23. Hamilton BS, Chung C, Cyphers SY, Rinaldi VD, Marcano VC, Whittaker GR. 2014. Inhibition of influenza virus infection and hemagglutinin cleavage by the protease inhibitor HAI-2. Biochem Biophys Res Commun 450:1070–1075.

24. Szabo R, Hobson JP, List K, Molinolo A, Lin C-Y, Bugge TH. 2008. Potent inhibition and global co-localization implicate the transmembrane Kunitz-type serine protease inhibitor hepatocyte growth factor activator inhibitor-2 in the regulation of epithelial matriptase activity. J Biol Chem 283:29495–504.

25. Wu SR, Teng CH, Tu YT, Ko CJ, Cheng TS, Lan SW, Lin HY, Lin HH, Tu HF, Hsiao PW, Huang HP, Chen CH, Lee MS. 2017. The Kunitz Domain i of Hepatocyte Growth Factor Activator Inhibitor-2 Inhibits Matriptase Activity and Invasive Ability of Human Prostate Cancer Cells. Sci Rep 7:1–19.

26. Wu SR, Lin CH, Shih HP, Ko CJ, Lin HY, Lan SW, Lin HH, Tu HF, Ho CC, Huang HP, Lee MS. 2019. HAI-2 as a novel inhibitor of plasmin represses lung cancer cell invasion and metastasis. Br J Cancer 120:499–511.

27. Roversi FM, Olalla Saad ST, Machado-Neto JA. 2018. Serine peptidase inhibitor Kunitz type 2 (SPINT2) in cancer development and progression. Biomed Pharmacother 101:278–286.

28. Jaimes JA, Millet JK, Goldstein ME, Whittaker GR, Straus MR. 2019. A Fluorogenic Peptide Cleavage Assay to Screen for Proteolytic Activity: Applications for coronavirus spike protein activation. J Vis Exp.

29. Straus MR, Whittaker GR. 2017. A peptide-based approach to evaluate the adaptability of influenza A virus to humans based on its hemagglutinin proteolytic cleavage site. PLoS One 12:e0174827.

30. Biacchesi S, Pham QN, Skiadopoulos MH, Murphy BR, Collins PL, Buchholz UJ. 2006. Modification of the trypsin-dependent cleavage activation site of the human metapneumovirus fusion protein to be trypsin independent does not increase replication or spread in rodents or nonhuman primates. J Virol 80:5798–806.

31. Galloway SE, Reed ML, Russell CJ, Steinhauer DA. 2013. Influenza HA Subtypes Demonstrate Divergent Phenotypes for Cleavage Activation and pH of Fusion: Implications for Host Range and

455 Adaptation. PLoS Pathog 9:e1003151.

456 32. Hatesuer B, Bertram S, Mehnert N, Bahgat MM, Nelson PS, Pöhlman S, Schughart K. 2013.
457 Tmprss2 Is Essential for Influenza H1N1 Virus Pathogenesis in Mice. PLoS Pathog 9:1–10.

458 33. Sakai K, Ami Y, Tahara M, Kubota T, Anraku M, Abe M, Nakajima N, Sekizuka T, Shirato K, Suzaki
459 Y, Ainai A, Nakatsu Y, Kanou K, Nakamura K, Suzuki T, Komase K, Nobusawa E, Maenaka K, Kuroda
460 M, Hasegawa H, Kawaoka Y, Tashiro M, Takeda M. 2014. The host protease TMPRSS2 plays a
461 major role in in vivo replication of emerging H7N9 and seasonal influenza viruses. J Virol
462 88:5608–16.

463 34. Baron J, Tarnow C, Mayoli-Nüssle D, Schilling E, Meyer D, Hammami M, Schwalm F, Steinmetzer
464 T, Guan Y, Garten W, Klenk H-D, Böttcher-Friebertshäuser E. 2012. Matriptase, HAT, and
465 TMPRSS2 Activate the Hemagglutinin of H9N2 Influenza A Viruses. J Virol 87:1811–1820.

466 35. Kühn N, Bergmann S, Kösterke N, Lambertz RLO, Keppner A, van den Brand JMA, Pöhlmann S,
467 Weiß S, Hummler E, Hatesuer B, Schughart K. 2016. The Proteolytic Activation of (H3N2)
468 Influenza A Virus Hemagglutinin Is Facilitated by Different Type II Transmembrane Serine
469 Proteases. J Virol 90:4298–4307.

470 36. Houser K, Subbarao K. 2015. Influenza vaccines: challenges and solutions. Cell Host Microbe
471 17:295–300.

472 37. Karlsson EA, Meliopoulos VA, van de Velde NC, van de Velde L-A, Mann B, Gao G, Rosch J,
473 Tuomanen E, McCullers J, Vogel P, Schultz-Cherry S. 2017. A Perfect Storm: Increased
474 Colonization and Failure of Vaccination Leads to Severe Secondary Bacterial Infection in Influenza
475 Virus-Infected Obese Mice. MBio 8.

476 38. Sielaff F, Böttcher-Friebertshäuser E, Meyer D, Saupe SM, Volk IM, Garten W, Steinmetzer T.
477 2011. Development of substrate analogue inhibitors for the human airway trypsin-like protease
478 HAT. Bioorganic Med Chem Lett 21:4860–4864.

479 39. Meyer D, Sielaff F, Hammami M, Böttcher-Friebertshäuser E, Garten W, Steinmetzer T. 2013.
480 Identification of the first synthetic inhibitors of the type II transmembrane serine protease
481 TMPRSS2 suitable for inhibition of influenza virus activation. Biochem J 452:331–343.
482 40. Yamaya M, Shimotai Y, Hatachi Y, Lusamba Kalonji N, Tando Y, Kitajima Y, Matsuo K, Kubo H,
483 Nagatomi R, Hongo S, Homma M, Nishimura H. 2015. The serine protease inhibitor camostat
484 inhibits influenza virus replication and cytokine production in primary cultures of human tracheal
485 epithelial cells. Pulm Pharmacol Ther 33:66–74.
486 41. Matsuyama S, Nagata N, Shirato K, Kawase M, Takeda M, Taguchi F. 2010. Efficient Activation of
487 the Severe Acute Respiratory Syndrome Coronavirus Spike Protein by the Transmembrane
488 Protease TMPRSS2. J Virol 84:12658–12664.
489 42. Gierer S, Bertram S, Kaup F, Wrensch F, Heurich A, Kramer-Kuhl A, Welsch K, Winkler M, Meyer B,
490 Drosten C, Dittmer U, von Hahn T, Simmons G, Hofmann H, Pohlmann S. 2013. The Spike Protein
491 of the Emerging Betacoronavirus EMC Uses a Novel Coronavirus Receptor for Entry, Can Be
492 Activated by TMPRSS2, and Is Targeted by Neutralizing Antibodies. J Virol 87:5502–5511.
493 43. Kinder JT, Klimyte EM, Chang A, Williams J V, Dutch RE. 2019. Human metapneumovirus fusion
494 protein triggering: Increasing complexities by analysis of new HMPV fusion proteins. Virology
495 531:248–254.
496 44. Hamilton BS, Gludish DWJ, Whittaker GR. 2012. Cleavage Activation of the Human-Adapted
497 Influenza Virus Subtypes by Matriptase Reveals both Subtype and Strain Specificities. J Virol
498 86:10579–10586.
499 45. Tse L V, Marcano VC, Huang W, Pocwierz MS, Whittaker GR. 2013. Plasmin-mediated activation
500 of pandemic H1N1 influenza virus hemagglutinin is independent of the viral neuraminidase. J
501 Virol 87:5161–9.
502

Figure Legends

Figure 1: Cleavage profile of the HMPV F: A fluorogenic peptide mimicking the cleavage site of HMPV F was incubated with the indicated proteases and cleavage was monitored by the increase of fluorescence at 390 nm.

Figure 2: Cytotoxicity assay to evaluate the cytotoxic effect of SPINT2.

293T cells were incubated with indicated SPINT2 concentrations for 24 hours. DMEM and 500 µM H_2O_2 served as controls. After 24 hours cell viability was determined via a spectrophotometric assay.

Figure 3: SPINT2 inhibits cleavage of HA protein expressed in 293T cells. Cells were transfected with plasmids encoding for the indicated HA and allowed to express the protein for ~18 hours. The recombinant proteases were incubated for 15 minutes with the indicated SPINT2 concentrations and subsequently added to the cells for 10 minutes (trypsin) or 90 minutes (matriptase and KLK5). Western bots were performed and the HA_1 band was quantified using ImageJ. (A) Quantification of the HA1 band comparing the signal intensity of the 0 nM SPINT2 samples against 10 nM and 500 nM SPINT2 of the respective HA/protease combination. (B – D) Western blots showing the cleavage of (B) A/Ca/04/09 H1N1 HA by matriptase and KLK5 at different SPINT2 concentration, (C) A/Aichi/2/68 H3N2 HA by KLK5 at different SPINT2 concentration and (D) A/Shanghai/2/2013 H7N9 HA by matriptase and KLK5 at different SPINT2 concentrations.

Figure 4: TMPRSS2, HAT, matriptase and KLK5 cleave HMPV F and SPINT2 is able to prevent cleavage by exogenous proteases. HMPV F was either expressed alone or co-transfected with protease and allowed to express for ~ 18hours. Cells were then metabolically starved of cysteine and methionine followed by radioactive S35 labeling of protein for 4 hours in the presence of TPCK-trypsin or specified protease. SPINT2 treated proteases were incubated at room temperature for 10 minutes and placed onto cells for 4 hours. Radioactive gels were quantified using ImageQuant software with percent cleavage equal to $\left[\left(\frac{F_1}{F_0+F_1}\right)x100\right]$. A and B) Co-transfected proteases TMPRSS2, HAT and matriptase are able to cleave

HMPV F while C and D) exogenous proteases KLK5 and matriptase but not KLK12 are able to cleave HMPV F. E and F) SPINT2 prevented cleavage of HMPV F by trypsin, KLK5 and matriptase at nm concentrations demonstrated by the loss of the F_1 cleavage product.

Figure 5: SPINT2 inhibits HA-mediated cell-cell fusion. VERO cells were transfected with plasmids encoding for (A) A/Ca/04/09 H1N1 HA or (B) A/Shanghai/2/2013 H7N9 HA and allowed to express the protein for ~18 hours. Recombinant matriptase and KLK5 were incubated with different SPINT2 concentrations for 15 minutes and then added to the HA-expressing cells for 3 hours. After 3 hours the cells were briefly treated with cell fusion buffer at pH5, washed, supplemented with growth medium and returned to the incubator for 1 hour to allow fusion. HA protein was detected using a fluorogenic Alexa488 antibody. Nuclei were stained using DAPI.

Figure 6: SPINT2 reduces viral growth in cell culture. MDCK cells were transfected with plasmids encoding for human matriptase or human TMPRSS2 and allowed to express the proteins for ~18 hours. Cells expressing human matriptase (B) or human TMPRSS2 (C) were then infected with A/Ca/04/09 H1N1 at a MOI of 0.1 and different SPINT2 concentration were added to each well. Non-transfected cells to which trypsin was added served as a control (A). (D) MDCK cells were infected with A/X31 H3N2 at an MOI of 0.1 and trypsin was added to assist viral propagation. Different SPINT2 concentration were added as indicated. After 48 hours of infection the supernatants were collected and used for an immuno-plaque assay to determine the viral loads. Experiment was repeated three times and each dot represents the viral titer of a single experiment. * indicates if $p = < 0.05$ compared to the sample with 0 nM SPINT2.

Figure 7: SPINT2 reduces viral growth when added 24 hours post infection. MDCK cells were infected with A/Ca/04/09 H1N1 at a MOI of 0.1 and trypsin was added. 500nM SPINT2 were added at the time of infection or 24 hours post infection. Supernatants were collected 48 hours post infection and used for an immuno-plaque assay to determine the viral titers.

Supplemental Figure 1: Fluorogenic peptides mimicking the cleavage sites (A) A/Ca/04/09 H1N1, (B) A/Japan/305/1957 H2N2 HA, (C) A/Aichi/2/68 H3N2 HA, (D) A/Vietnam/1203/2004 H5N1 LPAI HA, (E) A/Vietnam/1204/2004 H5N1 HPAI HA, (F) A/Taiwan/2/2013 H6N1 HA, (G) A/Shanghai/2/2013 H7N9 HA, (H) A/Hong Kong/2108/2003 H9N2 HA and (I) HMPV F were incubated with the indicated proteases and different SPINT2 concentrations. Cleavage was monitored by the increase of fluorescence at 390 nm and the resulting Vmax values were plotted against the different SPINT2 concentrations on a logarithmic scale (x-axis). Prism 7 software was then used to calculate the IC50 values based on the graphs shown in this figure as described in the "Material and Methods" section. In some cases the error bars are shorter than the height of the symbol and therefore are not displayed.

Table 1: IC50 values of all protease/peptide combinations. : Fluorogenic peptides mimicking the cleavage sites of A/Ca/04/09 H1N1, A/Japan/305/1957 H2N2 HA, A/Aichi/2/68 H3N2 HA, A/Vietnam/1203/2004 H5N1 LPAI HA, A/Vietnam/1204/2004 H5N1 HPAI HA, A/Taiwan/2/2013 H6N1 HA, A/Shanghai/2/2013 H7N9 HA, A/Hong Kong/2108/2003 H9N2 HA and HMPV F were incubated with the indicated proteases and different SPINT2 concentrations. Cleavage was monitored by the increase of fluorescence at 390 nm and the resulting Vmax values were used to calculate the IC50 values as described in the "Material and Methods" section. (A) IC50 values of influenza A fluorogenic cleavage site peptide mimics. Concentrations are in nanomolar. (B) IC50 values of the HMPV F cleavage site peptide mimic. Concentrations are in picomolar. NT = Not tested.

Table 2: Viral titers measured in the infection studies: Table shows the average viral titers and standard deviation calculated from the 3 independent biological replicates depicted in Figures 6 and 7. (A) Titers and standard deviation from infection studies shown in Figure 6. (B) Titers and standard deviation shown in Figure 7.

Table 1

A

	Trypsin	Matriptase	HAT	KLK5	KLK12	Plasmin
H1N1 HA	70.57	25	24.08	28.34	11.7	122.1
H2N2 HA	155.4	NT	34.74	8.269	6.881	NT
H3N2 HA	207.9	NT	15.33	9.537	NT	106
H5N1 HPAI HA	1135	194.1	NT	NT	NT	1166
H5N1 LPAI HA	145.8	5.316	23.56	6.375	3.656	160.1
H6N1 HA	30.52	NT	NT	29.93	14.04	NT
H7N9 HA	20.97	7.999	NT	NT	NT	77.59
H9N2 HA	99.16	9.015	12.74	11.79	NT	134

B

	Trypsin	Matriptase	HAT	KLK5	KLK12	Plasmin
HMPV F	40	0.3	NT	950	NT	NT

Table 2

A

SPINT2	Trypsin - H1N1		Matriptase - H1N1		TMPRSS2 - H1N1		Trypsin - X31	
(nM)	Average pfu/ml	StDev	Average pfu/ml	StDev	Average pfu/ml	StDev	Average pfu/ml	StDev
0	1.99E+08	3.91E+07	9.47E+06	9.02E+05	1.95E+09	4.39E+08	4.90E+08	1.16E+08
10	1.14E+08	3.70E+07	7.80E+06	1.04E+06	1.73E+09	2.95E+08	2.93E+08	7.57E+06
50	5.93E+07	3.06E+06	4.27E+06	1.40E+06	9.24E+08	4.16E+08	2.08E+08	6.16E+07
150	4.60E+07	8.72E+06	3.27E+06	1.62E+06	5.09E+08	2.44E+08	7.80E+07	4.65E+07
500	1.40E+07	5.29E+06	8.00E+05	5.29E+05	9.53E+07	3.43E+07	1.40E+07	5.29E+06

B

SPINT2	Trypsin - H1N1	
(nM)	Average pfu/ml	StDev
0	1.88E+08	1.06E+07
500	2.80E+07	1.00E+07
500 24hpi	4.07E+07	2.00E+07

582 **Figure 1**

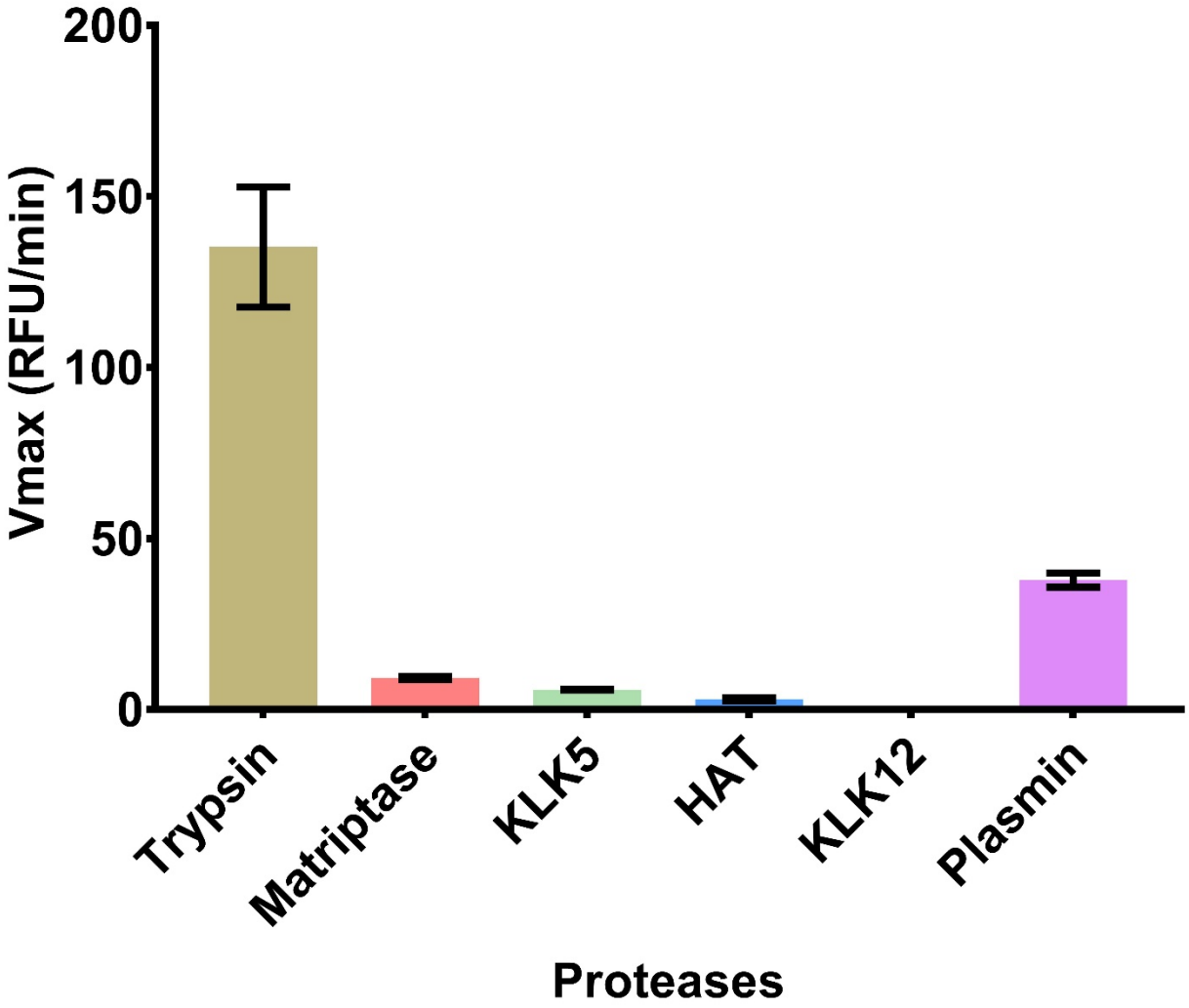

583

584 **Figure 2**

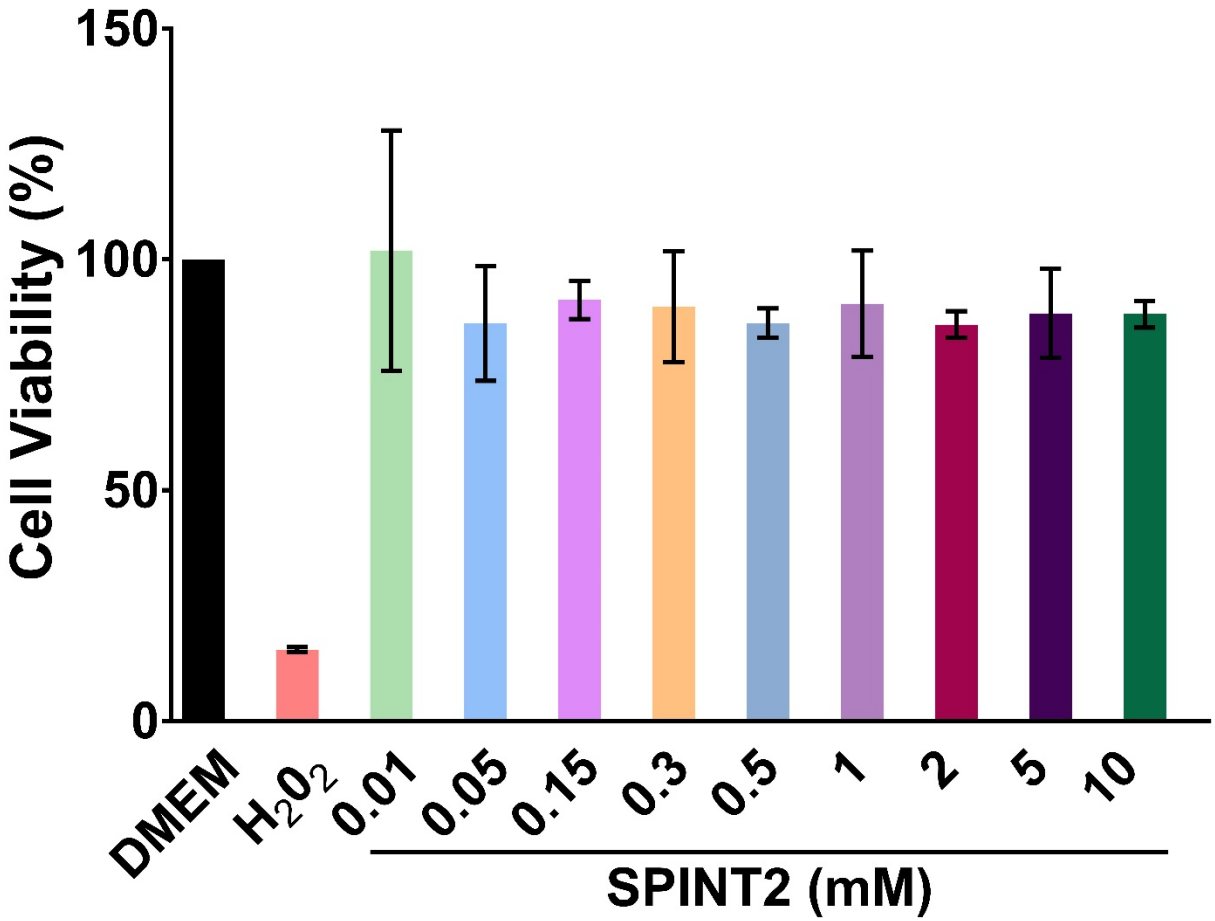

585

586

587 **Figure 3**

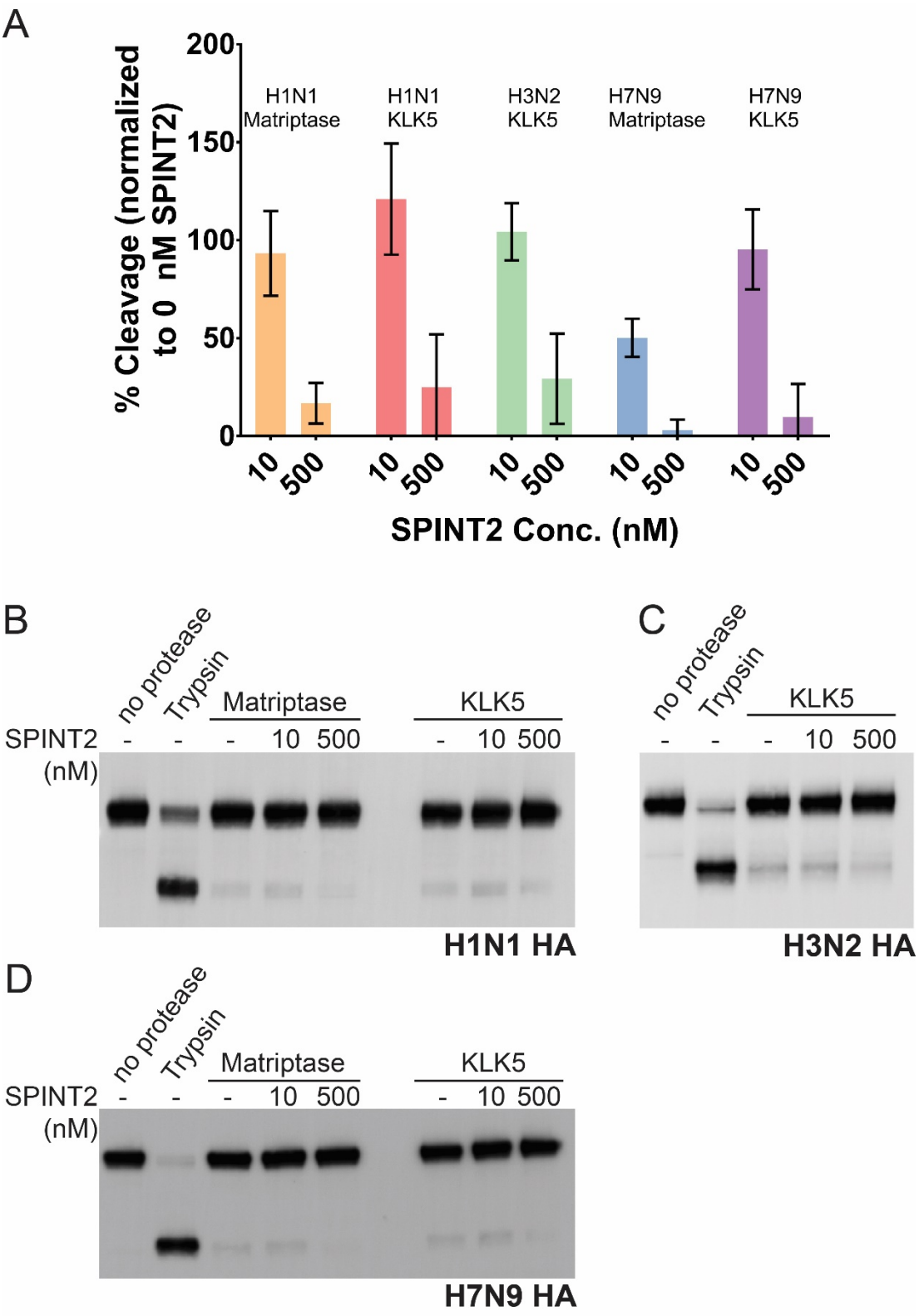

588

589

590 **Figure 4**

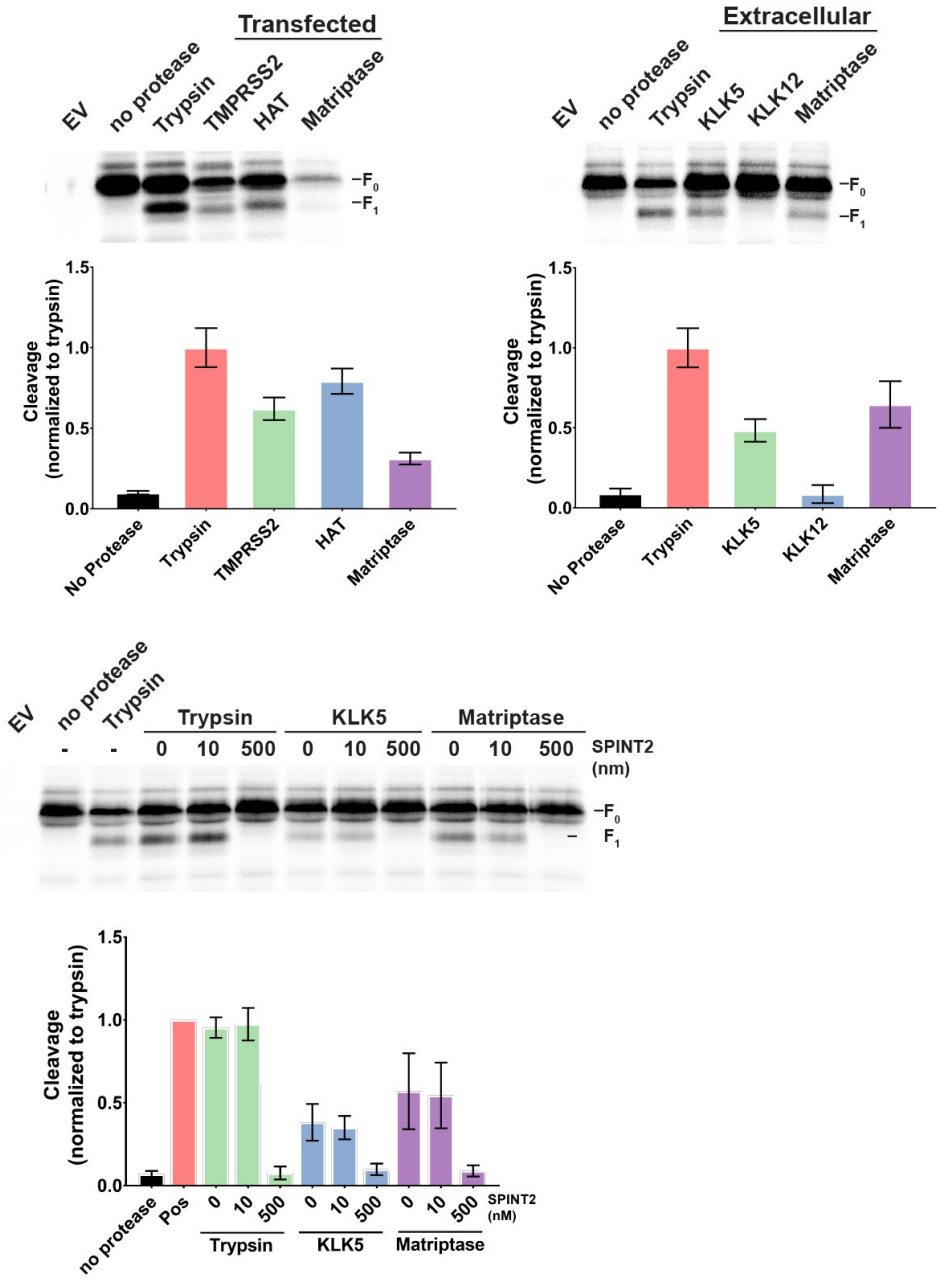

591

592

593 **Figure 5**

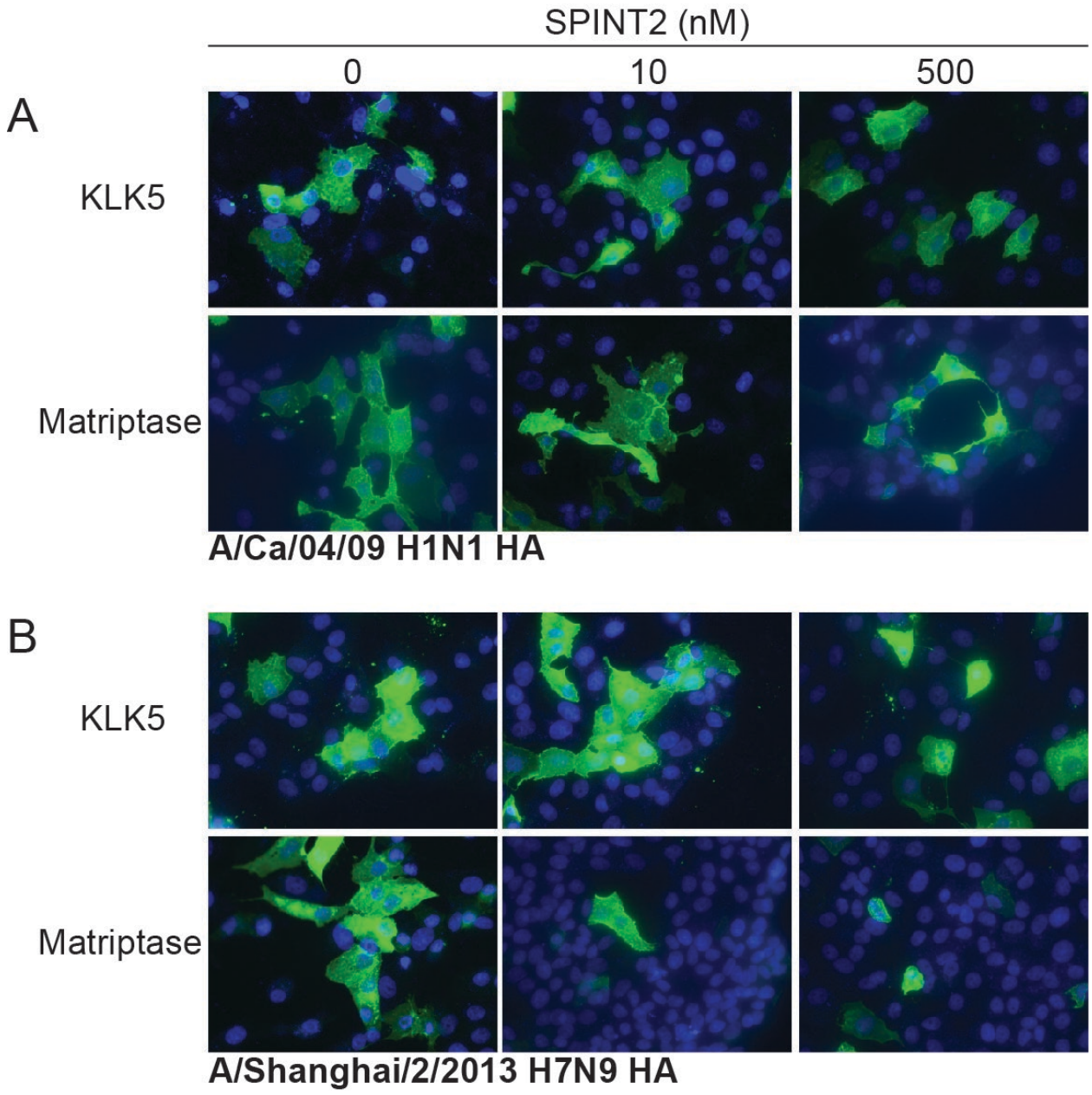

594

595

596 **Figure 6**

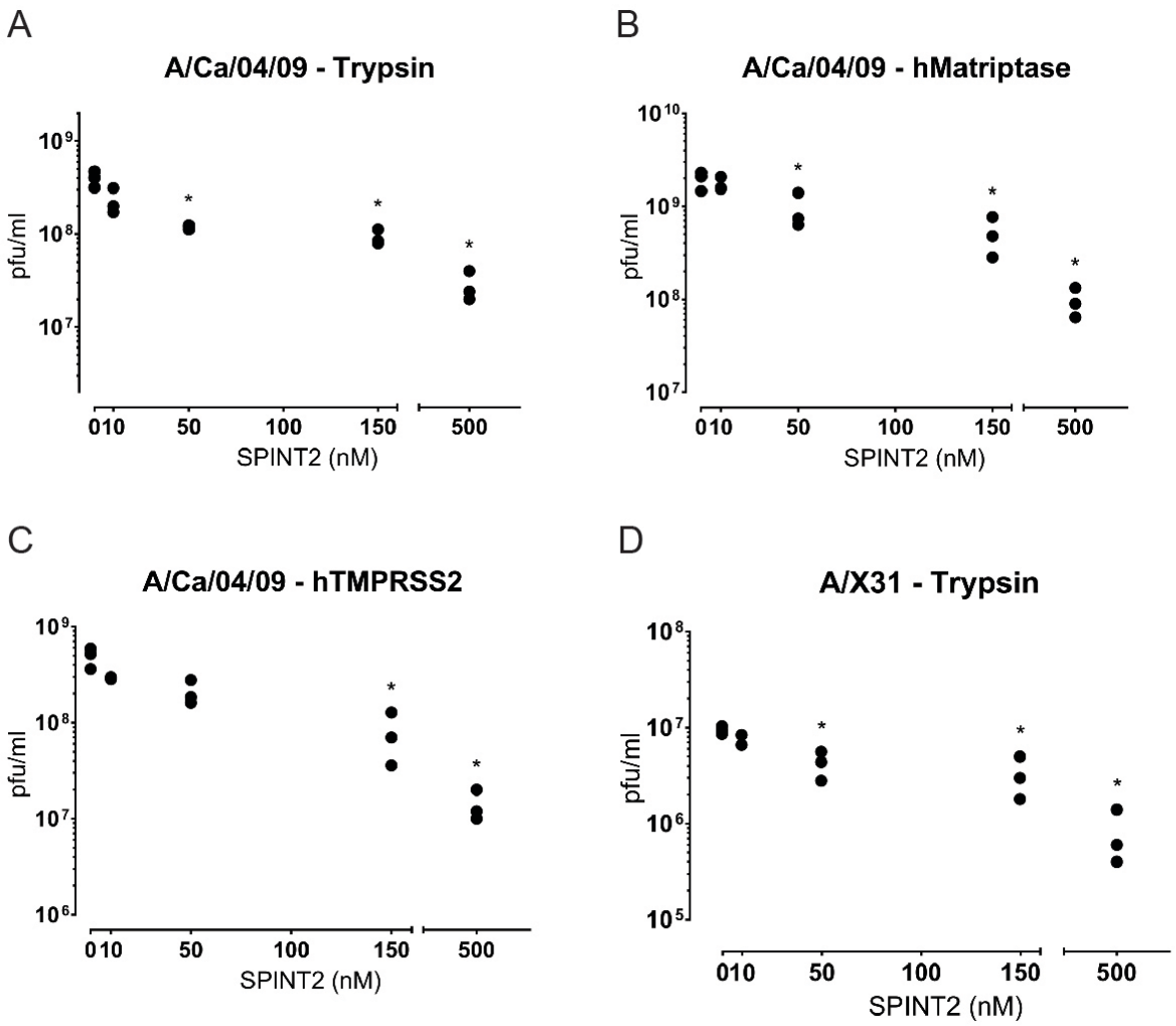

597

598

599 **Figure 7**

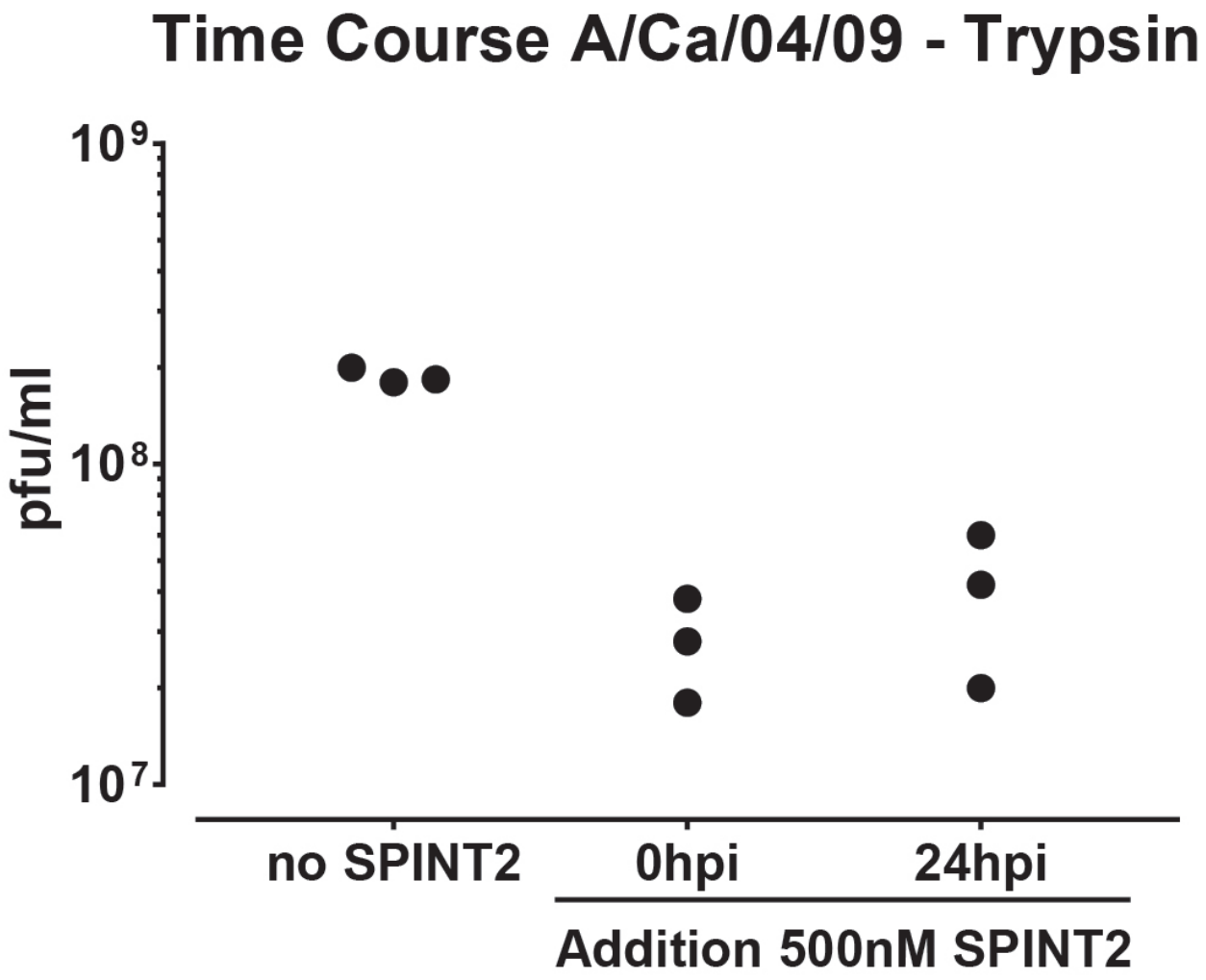

600

601

602 **Supplemental Figure 1**

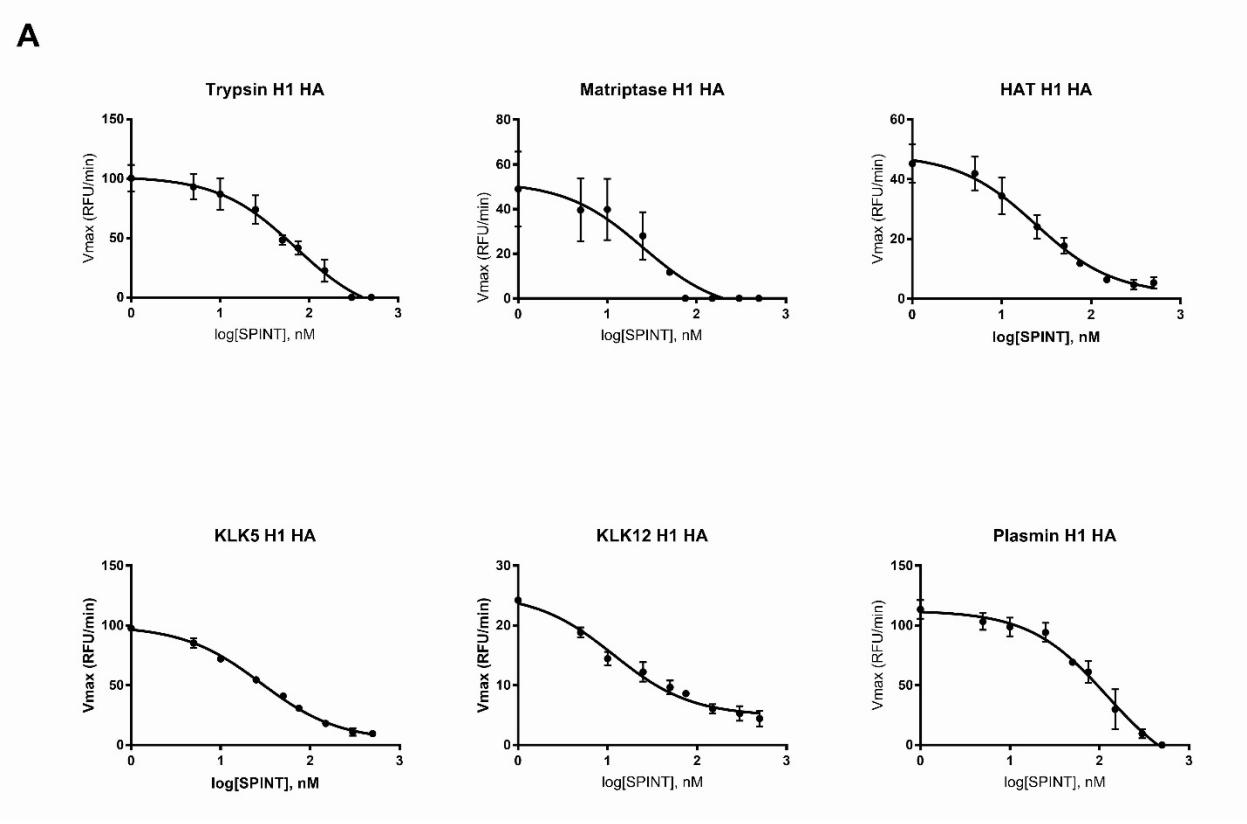

603

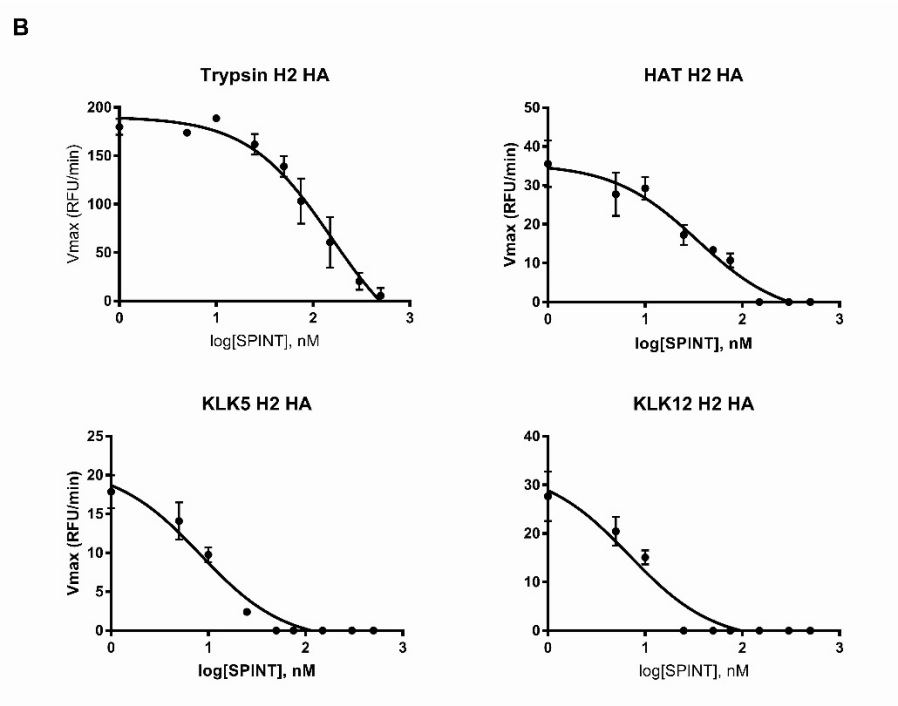

604

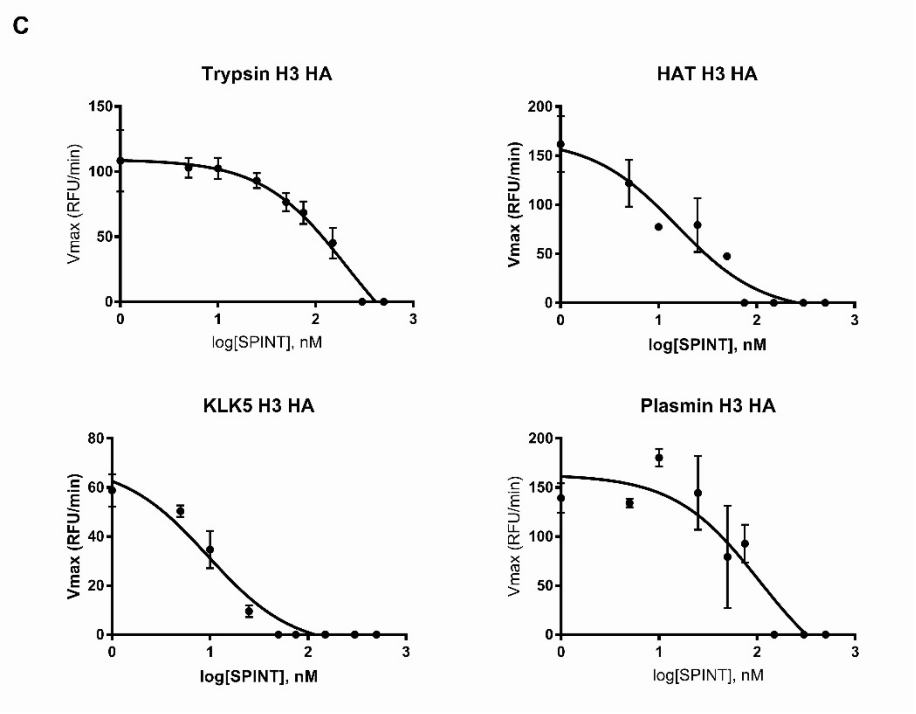

605

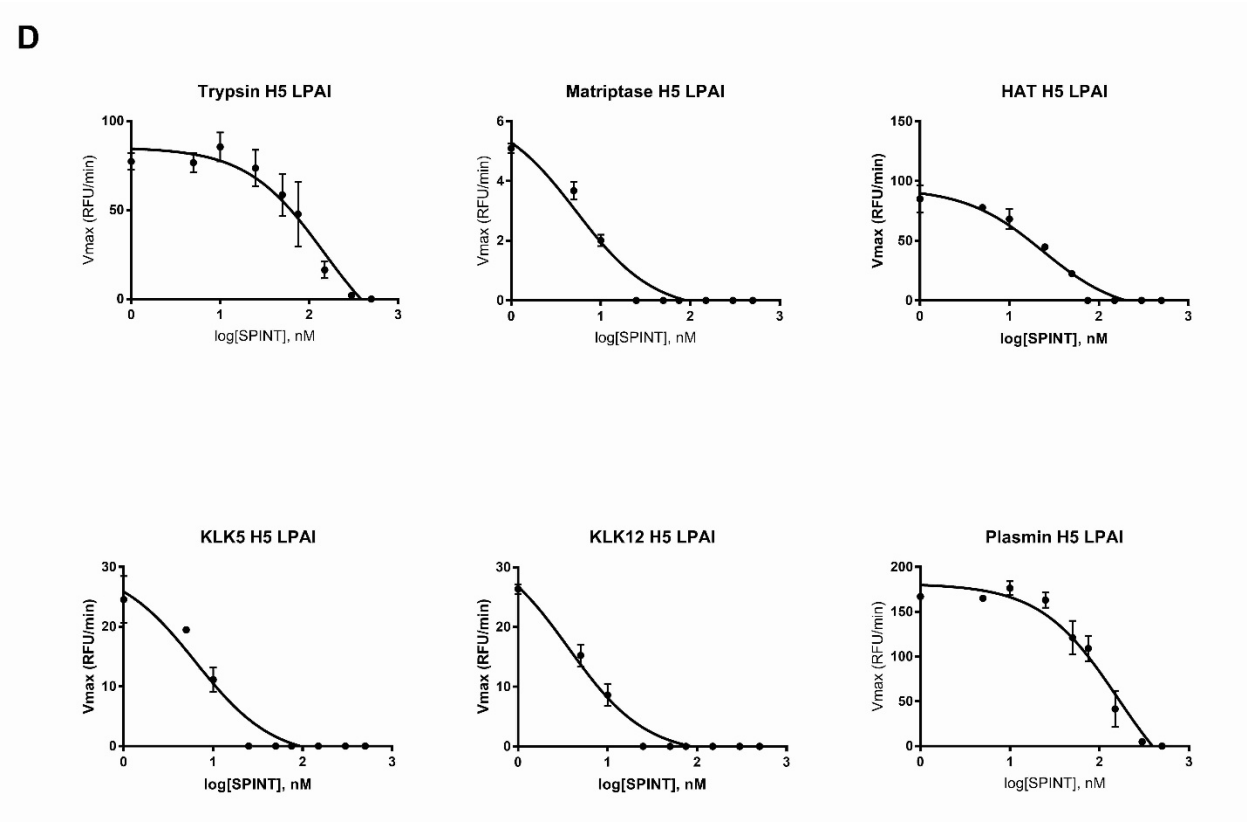

606

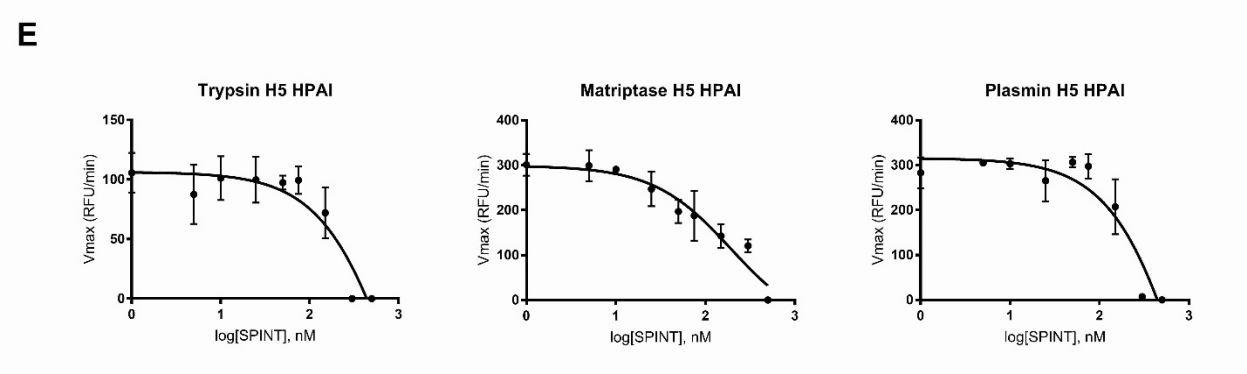

607

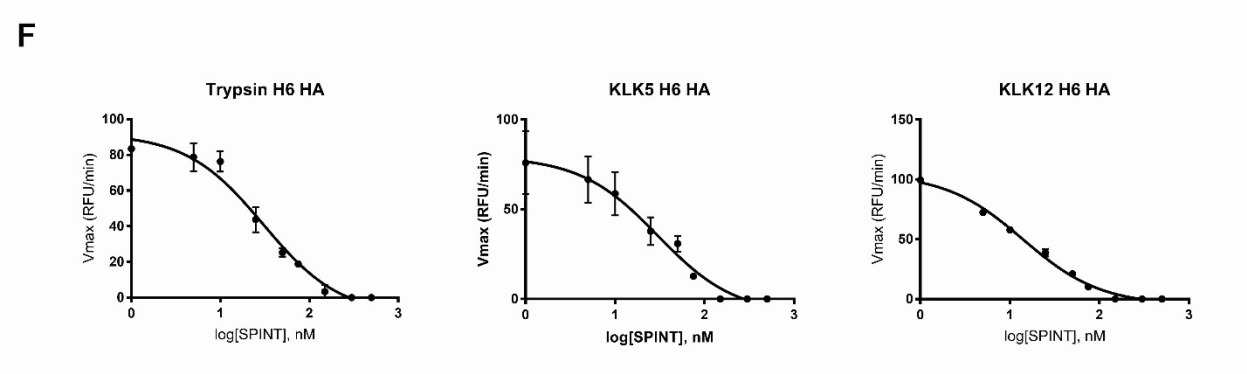

608

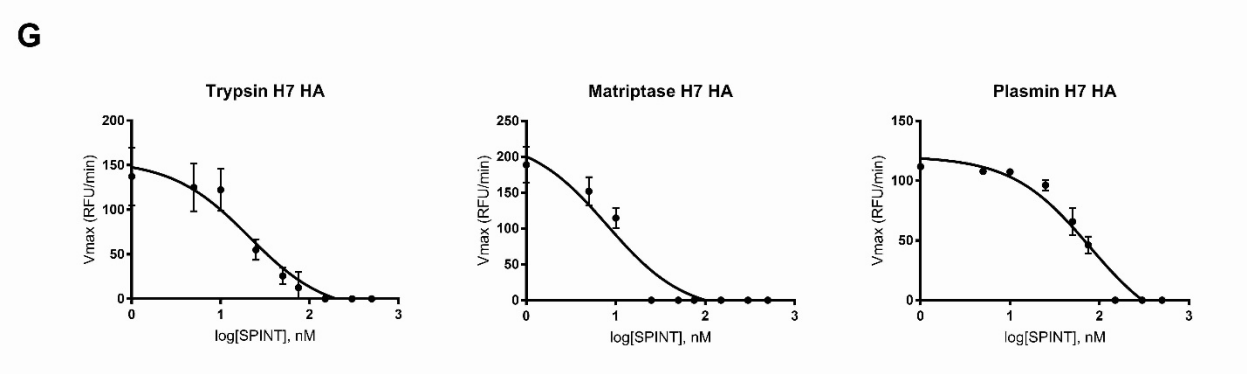

609

H

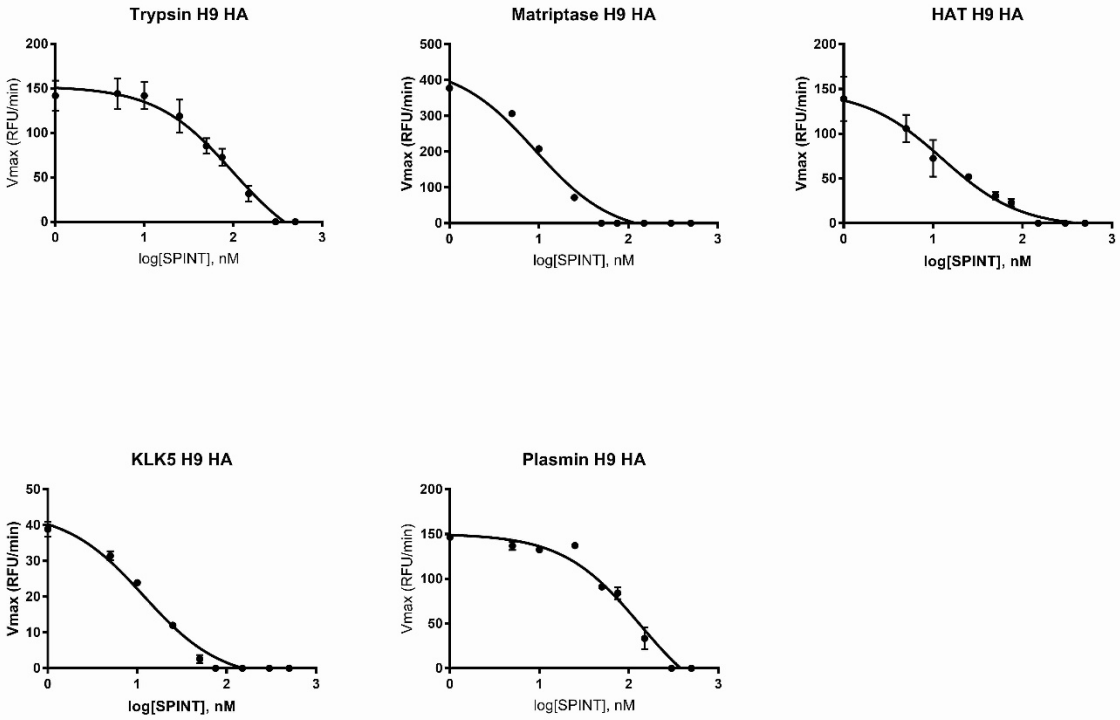

610

I

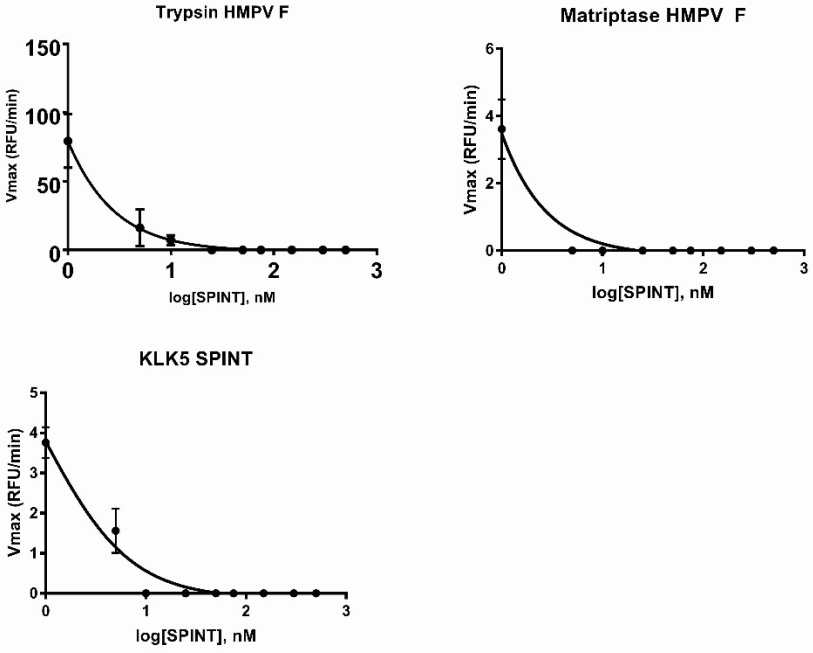

611